SERDP

INTERIM REPORT II

Object Burial by High-Energy Forcing: Liquefaction and Granular Sorting

Sarah E. Rennie
Alan Brandt
Johns Hopkins University Applied Physics Laboratory

January 2021

SERDP Project MR19-1126

REPORT DOCUMENTATION PAGE

Form Approved
OMB No. 0704-0188

1. REPORT DATE *(DD-MM-YYYY)*	2. REPORT TYPE	3. DATES COVERED *(From - To)*
31/01/2021	SERDP Interim Report	4/9/2019 - 4/8/2022

4. TITLE AND SUBTITLE
Object Burial by High-Energy Forcing: Liquefaction and Granular Sorting

Interim Report II

5a. CONTRACT NUMBER
19-C-0015

5b. GRANT NUMBER

5c. PROGRAM ELEMENT NUMBER

6. AUTHOR(S)
Sarah E. Rennie
Alan Brandt

5d. PROJECT NUMBER
MR19-1126

5e. TASK NUMBER

5f. WORK UNIT NUMBER

7. PERFORMING ORGANIZATION NAME(S) AND ADDRESS(ES)
Johns Hopkins University Applied Physics Laboratory
11100 Johns Hopkins Road
Laurel, MD 20723

8. PERFORMING ORGANIZATION REPORT NUMBER
FPS-R-20-0685

9. SPONSORING/MONITORING AGENCY NAME(S) AND ADDRESS(ES)
Strategic Environmental Research and Development Program
4800 Mark Center Drive, Suite 17D03
Alexandria, VA 22350-3605

10. SPONSOR/MONITOR'S ACRONYM(S)
SERDP

11. SPONSOR/MONITOR'S REPORT NUMBER(S)
MR19-1126

12. DISTRIBUTION/AVAILABILITY STATEMENT
DISTRIBUTION STATEMENT A. Approved for public release: distribution unlimited.

13. SUPPLEMENTARY NOTES

14. ABSTRACT

This review and status report is focused on the potential for burial or possible exhumation of unexploded ordnance (UXO1) and marine munitions in sandy coastal areas by high energy wave forcing. Several processes for UXO burial have been included in the Underwater Munitions Expert System (UnMES), most notably burial by scour. Some evidence suggests that, in the nearshore and surf zone, high energy waves could also drive burial by liquefaction or by granular sorting. These mechanisms have been reviewed for inclusion in UnMES as process models. It has been found that the extant literature on the behavior of isolated objects, relevant to munitions burial, by these mechanisms is highly limited. While studies of the behavior of coastal structures, e.g. pipelines, breakwaters, under liquefaction can be extrapolated to objects, validation of such extrapolations is limited, and they lack general applicability to sandy sediments. The main objective of this report is to determine whether a new liquefaction model should be included in the current version of UnMES which is focused on sandy environments. Currently funded SERDPMRefforts are designed to address high-energy burial mechanisms; however, at present these studies are still in progress. As a result, there remains an insufficient level of understanding, as well as a lack of adequate data to justify inclusion of these processes in UnMES. Thus, the decision to not include new physics-based liquefaction and granular sorting models in the expert system at this time is appropriate(a NO-GO decision). For research purposes however, a simplified liquefaction burial model, discussed in this report, is currently implemented in UnMES as a preliminary, exploratory tool. At some future time, with increased knowledge and data, a validated model for high-energy burial in non-cohesive sediment would be an important addition to UnMES.

15. SUBJECT TERMS
Underwater Munitions, Object Burial, High-Energy Forcing, Liquefaction, Granular Sorting, UXO, UXO mobility, Bayesian Model of Munition Behavior, computer based expert system UnMES

16. SECURITY CLASSIFICATION OF:			17. LIMITATION OF ABSTRACT	18. NUMBER OF PAGES	19a. NAME OF RESPONSIBLE PERSON
a. REPORT	b. ABSTRACT	c. THIS PAGE			Sarah Rennie
UNCLASS	UNCLASS	UNCLASS	UNCLASS	29	19b. TELEPHONE NUMBER *(Include area code)* 443-778-8178

Object Burial by High-Energy Forcing: Liquefaction and Granular Sorting

S.E. Rennie, A. Brandt
Johns Hopkins Applied Physics Laboratory

November 2020

Table of Contents

Acronyms and Symbols

BN	–	Bayesian Network
B_{obj}	–	Burial depth of the UXO
CPT	–	Conditional Probability Table(s)
d	–	water depth
e	–	void ratio
D_{obj}	–	Diameter of the UXO
D_r	–	Relative Density of the sediment
f_c	–	Friction coefficient
FRF	–	Field Research Facility, USACE, Duck, North Carolina
h	–	thickness of sediment layer
H_s	–	Significant wave height
G	–	shear modulus of the sediment
k	–	hydraulic conductivity
L	–	wave length
MC	–	Monte Carlo
MR	–	Munitions Response
n	–	porosity
P_b	–	Pressure at the seabed
SERDP	–	Strategic Environmental Research and Development Program
S_{obj}	–	Specific gravity of the UXO
S_r	–	Saturation ratio of the pore water
S_{sed}	–	Specific gravity of the bulk sediment
S_{water}	–	Specific gravity of water
T	–	wave period
UnMES	–	Underwater Munitions Expert System
UXO	–	Unexploded Ordnance
z_L	–	liquefaction depth
β	–	compressibility of pore fluid
γ	–	unit weight
μ	–	viscosity
ν	–	Poisson ratio
σ	–	stress

Object Burial by High-Energy Forcing: Liquefaction and Granular Sorting

Abstract

This review and status report is focused on the potential for burial or possible exhumation of unexploded ordnance (UXO[1]) and marine munitions in sandy coastal areas by high energy wave forcing. Several processes for UXO burial have been included in the Underwater Munitions Expert System (UnMES), most notably burial by scour. Some evidence suggests that, in the nearshore and surf zone, high energy waves could also drive burial by liquefaction or by granular sorting. These mechanisms have been reviewed for inclusion in UnMES as process models. It has been found that the extant literature on the behavior of isolated objects, relevant to munitions burial, by these mechanisms is highly limited. While studies of the behavior of coastal structures, e.g. pipelines, breakwaters, under liquefaction can be extrapolated to objects, validation of such extrapolations is limited, and they lack general applicability to sandy sediments. The main objective of this report is to determine whether a new liquefaction model should be included in the current version of UnMES which is focused on sandy environments. Currently funded SERDP-MR efforts are designed to address high-energy burial mechanisms; however, at present these studies are still in progress. As a result, there remains an insufficient level of understanding, as well as a lack of adequate data to justify inclusion of these processes in UnMES. Thus, the decision to not include new physics-based liquefaction and granular sorting models in the expert system at this time is appropriate(a NO-GO decision). For research purposes however, a simplified liquefaction burial model, discussed in this report, is currently implemented in UnMES as a preliminary, exploratory tool. At some future time, with increased knowledge and data, a validated model for high-energy burial in non-cohesive sediment would be an important addition to UnMES.

1. High-Energy Forcing: Introduction

The underwater munitions expert system UnMES is based upon a Bayesian Network construct, a useful method of modeling systems with complex relationships in a probabilistic manner, where each relationship is characterized by a conditional probability table (CPT). A common approach to building a Bayesian network is to train the CPT using a dataset of example cases. As an alternative, due to the limited amount of field and laboratory data applicable to UXO burial and mobility, simple deterministic models that capture the first-order physics of the processes of interest have been developed. Extensive Monte Carlo (MC) simulations employing these models are run over the relevant combinations of input variable ranges in order to populate the CPTs in UnMES [Rennie *et al.,* 2019]. UXO at sites of concern have generally been deposited over an

[1] Here we use UXO as a generic term representing all objects if interest for remediation on or buried in the coastal ocean, including marine munitions, flares, etc. that may have been fired, dumped or otherwise deposited.

extended time period (months to years) and over an area that encompasses different bathymetric and hydrodynamic regimes (from deep water to the beach face). The spatial application of UnMES partitions the site into provinces that have similar sediment and water depth characteristics. UnMES, as currently implemented, focuses on the time scale of a single storm event, as storms are the primary drivers of burial and migration events.

Burial and re-exposure of bottom sitting objects (UXO, and marine munitions in general) during high-energy wave conditions, such as present in the surf zone and in the nearshore coastal region during a storm, wherein the seabed can be affected by pressure fluctuations due to the presence of surface waves, can be controlled by mechanisms different than scour and bedform migration that occur under less energetic conditions. Two high-energy mechanisms of specific interest are liquefaction and granular sorting, which require a clear hydrodynamic and geodynamic understanding to explicate. In geotechnical terms, liquefaction refers to the sediment state under cyclic forcing wherein overburden pressure variations result in the loss of vertical effective stresses, so that the water-sediment mixture behaves like a fluid. This type of response is sometimes called fluidization. Granular sorting refers to a range of phenomena where granular material exhibits circulation patterns similar to fluid convection when subjected to shaking or vibration. Both these mechanisms can result in object burial depth considerably greater than the body diameter, or alternatively cause re-exposure of objects from great depths if the UXO are sufficiently less dense than the surrounding media.

2. The Liquefaction Process

Soil liquefaction occurs when a saturated or partially saturated soil substantially loses strength and stiffness in response to an applied stress, such as shaking during an earthquake or large amplitude surface waves, that causes excess pore pressure and decreased effective stresses. Under these conditions, part of the seabed can become unstable, the effective stresses between the sediment grains disappear and the water-soil mixture behaves like a liquid.

To a large extent studies of liquefaction have focused on earthquake forcing and its effects on gravity structures (e.g. buildings, breakwaters, bridge piers) and on buried pipelines [Sumer, 2014a]. Liquefaction under waves (the process most relevant to UXO burial) that alternately increase and decrease the pressure on the bedform has also been of interest primarily due to their effect on pipelines and to a limited extent on individual objects which is the situation of interest for UnMES.

Over the past several decades, much research into wave-soil-structure interaction has been conducted by geotechnical engineers in an effort to understand the cause of damage observed at coastal structures (breakwaters, pipelines, etc.), as well as the subsidence of concrete blocks used to armor the seabed. Analyses identify wave-induced shear failure and liquefaction as the two

important damaging mechanisms, with liquefaction dominant in non-cohesive sediments [Jeng, 2003] . The passage of an ocean wave generates significate dynamic pressure on the seabed below, that is a maximum under the wave crest and minimum below the trough as illustrated in Figure 2.1.

Early work employing both analytical and numerical models have been proposed to consider pore-fluid-sediment interaction. The first studies modeling liquefaction assumed that both the fluid and the sediment are incompressible, an uncoupled approach that is appealing for application within UnMES. If a simplified explanation is sufficient to capture enough of the response, that is the preferred process model to use in the expert system, because it is assumed that in an operational setting, there will not be enough detailed environmental data to justify applying a more complicated model. However, it turns out that the liquefaction response in medium to fine sands depends on the coupling of pore-fluid motion and the soil during contraction and expansion. Therefore, applicable liquefaction models are based on the classical poro-elasticity theory [Biot, 1956]. For these models, the sediment is assumed to be a poro-elastic medium where the voids in the soil skeleton are filled with water. A summary of the Biot consolidation equations, including derivation and example solutions is presented in Sumer [2104a, Ch. 2].

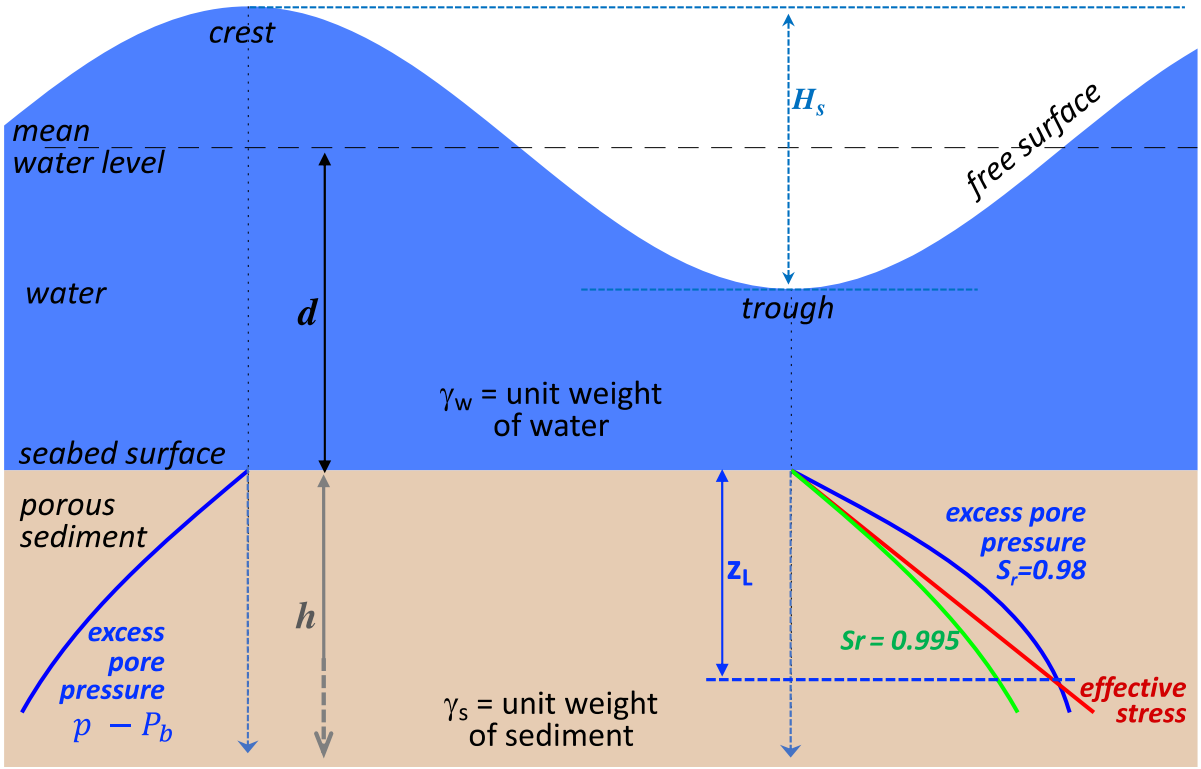

Figure 2.1 Diagram of wave-seabed interaction showing factors influencing momentary liquefaction (adapted from Jeng [2003] and Qi and Gao [2018]).

Wave-driven liquefaction is generally classified into two different mechanisms: residual (progressive), and momentary (oscillatory), depending on how the excess pore pressure is generated [Sumer, 2014a]:

1. For the residual mechanism, $\overline{P}$, the pressure resulting from cyclic loading of loosely-packed soil generates shear stresses, generating, in-turn, contraction of the pore volume and accumulating buildup of pore-water pressure, especially if drainage is impeded.

2. Momentary liquefaction, $\widetilde{|P|}$, appears as an oscillatory response to each wave related to the phase lag in pore pressure with depth into the seabed. Under the wave trough, the pore fluid has an upward-directed vertical pressure gradient ($\frac{dp}{dz} < 0$). If the soil is completely saturated, the pressure gradient is small, but for unsaturated soils, the presence of air allows the pore pressure to be dissipated very quickly, and $\frac{dp}{dz}$ can be quite large near the seabed surface. Figure 2.1 illustrates the distribution of transient excess pore pressure at the moment of passage of the wave.

In essence, momentary liquefaction describes the elastic response under an individual wave event while residual determines the net overall (plastic) effect of the continuous build-up of pore pressure due to successive waves. Momentary and residual liquefaction are in effect different aspects of the same process. Generally, in order to simplify analysis, these two components of excess pore pressure have been studied and modeled independently. In reality, the two mechanisms can both be present or even coupled. Jeng *et al.* [2007] suggested a weighting factor $\varepsilon = \frac{\bar{P}}{|P|}$, to assess the relative contributions and clarify the applicable ranges of the residual and momentary mechanisms. Multiple aspects of both wave and sediment characteristics are factors in determining the relative contributions. High relative soil density, a large coefficient of consolidation, as well as low saturation ratio, enhance the oscillatory response [Sumer, 2014a]. The current version of UnMES focuses on sandy coastal conditions, where the momentary component $\widetilde{|P|}$ is dominant, therefore the following examination considers only wave-induced momentary liquefaction. The dependence of liquefaction response to varying sediment characteristics is discussed further in the Section 2.2.

2.1 Liquefaction Modeling

To understand wave-induced seabed response based on Biot's poro-elastic theory, a system of four governing equations must be solved: an assumed constitutive law, an overall equilibrium equation, an equation representing the equilibrium of pore fluid flow, and the mass balance [Jeng, 2003]. A series of papers by Hsu and Jeng (Hsu *et al.*, 1993; Hsu and Jeng, 1994) defined the set of equations in terms of sediment structure properties:

1) the wave-induced pore pressure in the sediment, p

2) the soil displacements in the horizontal and vertical directions (or, equivalently, the effective normal stresses in those directions, $\sigma_x', \sigma_y', \sigma_z'$)

3) shear stresses, τ'_{ij}

Hsu *et al.* [1993] then obtained a direct analytical solution satisfying the boundary conditions provided by the forcing progressive wave over a porous bed of infinite thickness (h = ∞). The closed form solution required a complex mathematical presentation, which becomes even more complicated when solving for a finite sediment layer depth [Hsu and Jeng, 1994]. This framework has been adapted and applied to a number of situations (e.g., Jeng, [1997]), including the SERDP field experiment DUCK15 by Klammler *et al.* [2020], discussed in Section 2.3.

Alternatively, simpler solutions can be found using a boundary layer approximation [Mei and Foda, 1981] which is suitable for engineering applications such as UnMES. A 2-D version of the direct analytical solution for h = ∞ was formulated by Yamamoto *et al.* [1978] which has compared well to experimental data in coarse and fine sands. Zen and Yamazaki [1990] argued that a 1-D approach can be used for the case of relatively long waves, and the 1-D approximation of Chowdhury [2006] was shown by Qi and Gao [2015] to agree reasonably with the Yamamoto solution.

To specify the maximum depth, z_L, to which liquefaction conditions extend, it is necessary to define the portion of the solution representing sediment instability. Solutions can be examined based on several different proposed criteria. The most common criteria used to determine transition into a liquefied state are:

A) loss of vertical effective normal stress, when the effective normal stress σ'_z is greater than the submerged weight of the soil: $-(\gamma_s - \gamma_w)z - \sigma'_z \leq 0$,

B) excess pore pressure when the excess pore pressure is greater than the overburden soil pressure: $-(\gamma_s - \gamma_w) + (P_b - p) \leq 0$,

where P_b is the wave pressure at the surface of the seabed. Maximum P_b (amplitude) of pressure exerted on the bed is:

$$P_{b(max)} = \gamma_w H_s \frac{1}{2\cosh(\lambda d)},$$

with H_s the wave height, d the water depth, and λ the wavenumber ($\lambda = {}^{2\pi}/_{L}$); L being the wavelength.

Another criterion for momentary liquefaction was defined as the vertical seepage force acting on the soil [Qi and Gao, 2015]:

C) pore-pressure vertical gradient: $-(\gamma_s - \gamma_w) - \frac{dp}{dz} \leq 0$.

Criterion C expresses the momentary state under a wave trough when the upward-directed vertical gradient of excess pore-pressure becomes larger than the buoyant weight of the soil, destabilizing the seabed, leading toward a liquefied state. All of these criteria describe how wave-induced

pressure changes interact with the pressure supplied by the overlaying sediment and their calculation depends on both sediment and wave properties.

Recent investigations into liquefication phenomena have proposed use of a liquefaction degree, indicating a ratio of the destabilizing to the stabilizing forces, $R = \frac{excess\ pore\ pressure}{stablizing\ force}$, rather than a fixed threshold (Qi and Gao [2018], Klammler *et al*. [2021]). This relationship conceptualizes the soil response as a fully liquefied layer where $R = 1$, beneath which there is a partially-destabilized region where a portion of the mean initial effective sediment stress has been compensated by excess pore pressure.

For the prototype version of UnMES, UXO response is modeled as occurring over the course of an individual large storm event, a sequence of many hours [Rennie *et al.,* 2019]. It is likely that only during the peak of a storm will waves be large enough to destabilize the sediment down to significant depths (deeper than the UXO diameter); however, studies show that under the right conditions, onset of liquefaction can occur within minutes [Sumer *et al.,* 1999, Klammler *et al.,* 2020]. The question then becomes how rapidly does the UXO sink down through the liquefied region (discussed in Section 2.3). Commonly, UXO have been present on the seabed at remediation sites for an extended period (up to decades); or that some number of years have passed since the last site survey. During a long time period it is likely that several large amplitude storm events occurred which could cumulatively contribute to liquefaction burial. Therefore, the history of storms affecting the site is of interest. Clearly, in addition to knowledge about the sediment, information about regional storm amplitude and duration will be needed to accurately model burial driven by liquefaction.

2.2 Sediment and Pore Water Characteristics

For both numerical and analytic solutions for wave-seabed interaction, important parameters include a number of sediment characteristics that affect the magnitude and distribution of pore-pressure buildup. For the prototype UnMES that focuses on predicting UXO burial at sandy coastal sites, the most relevant range of soil characteristics relates to the properties of fine to medium sand. Important factors include both hydraulic properties such as permeability and mechanical properties, for example the shear modulus. Some of these properties are known to be fairly constant values for a given soil type, but several can vary significantly and are often not well known, requiring specialized geomechanical testing to determine. For operational application of the expert system UnMES for remediation guidance, there may be limited ability to obtain detailed soil measurements. Within UnMES, which takes a probabilistic approach in order to make useful predictions even in the face of uncertainty, the expected range of these environmental factors can be included as part of the input information.

Permeability describes how easily the pore fluid can move through the soil and is a property of the pore space geometry. It is usually expressed as hydraulic conductivity, k, with units of velocity after taking into account fluid viscosity and density, which for our purposes can be considered constant. Sometimes referred to as the coefficient of permeability, a representative value for fine sand is $k = 1x10^{-4}$ m/s, while gravel can have k as large as $1x10^{-2}$ m/s. In silty clays hydraulic conductivity can be smaller than $1x10^{-6}$ m/s. In some applications, possible anisotropy of the pore space geometry is considered, and hydraulic conductivity is represented by horizontal k_x and vertical k_z coefficients [Klammler *et al*., 2020].

The rigidity of the soil skeleton, or its response to shear deformation, is quantified by the sediment shear modulus G, the proportionality coefficient in the shear stress-shear strain relationship. In fine sand, G is usually on the order of $1x10^7$ N/m^2, but the presence of silt or clay can greatly reduce that value. In studies of residual liquefaction in coarse silt, Sumer *et al.* [1999] reported G = $5x10^5$ N/m^2. Very dense sand can have a value of G as high as $5x10^8$ N/m^2 [Sumer, 2014a]. In many formulations, Young's modulus of soil elasticity E is used in place of G, with E related to G as $E = 2G(1 + \nu)$; ν being the Poisson ratio, another material property describing the expansion or contraction of the sediment in the direction perpendicular to loading. For a sandy soil, the common value of ν is 0.33, and ν exhibits only a small range, generally between 0.3 to 0.4 [Sumer, 2014a].

The soil overburden pressure depends on the bulk density of the sediment, a function of the porosity, n, the percentage of pore volume, or fraction of voids in the total volume. In sand, porosity n ranges from 0.2 to 0.5, being mostly commonly between 0.3 to 0.4. An alternate metric for the fraction of voids is the void ratio e, the ratio of the void fraction to the volume of solids, so that $e = n/(1- n)$. The measure "relative density" or D_r (not to be confused with specific density) is sometimes used in studies to describe how densely packed the sand bed is, capturing information about both the porosity and the permeability where $D_r = (e_{max} - e)/ (e_{max} - e_{min})$. Loosely packed granular soils have D_r less that 50%, while very dense beds may have D_r as high as 85%. At some locations, D_r can vary with time: strong wave action will generally pack the sand near the surface of the seabed to $D_r > 65\%$, but following a long period of calm, bioturbation can cause a reduction in D_r [Jackson and Richardson, 2007].

It is difficult to accurately determine n and D_r from sample cores due to disturbance of the sediment. Specialized sedimentological tests are required in order to measure the maximum and minimum void ratios, e_{max} and e_{min}. Methods of inferring sediment properties from high-frequency acoustic measurements are being improved [Jackson and Richardson, 2007] and offer the great advantage of rapid wide area coverage, compared to laborious box coring by divers. Acoustic tracks have revealed substantial spatial heterogeneity in sediment density.

One of the most important factors in determining the onset of momentary liquefaction is the presence of undissolved air or gas in the pore water, which strongly affects its compressibility. The degree of saturation S_r, is the ratio of volume of water to the volume of voids, with $S_r = 1.0$ indicating complete saturation (no air/gas content). The presence of a very small amount (< 1%) of air/gas dramatically increases the pore-water water dissipation with depth, which increases $\frac{dp}{dz}$ (lift under the wave trough). In Figure 2.1 two profiles of excess pore pressure (p - P_b) are modeled as in Qi and Gao [2015]: the blue line shows p with 2% gas content ($S_r = 0.98$), while the green profile is p for a highly saturated pore fluid ($S_r = 0.995$). Only for the unsaturated conditions does p - P_b exceed the effective stress due to the weight of the soil overburden. This is because compressibility of the pore fluid, β, is influenced by saturation degree as $\beta = \frac{1}{K_w} + \frac{1-S_r}{P_{w0}}$ where K_w is the elastic bulk modulus of seawater (a constant ~= $2x10^9$ Pa) and P_{w0} is the atmospheric pressure level. The strong effect of S_r on momentary liquefaction is also plotted in Figure 2.2a.

In some natural settings, a small amount of gas content is likely to be present in the seabed, with field observations reported up to 6% ($S_r = 0.94$) in an area where large tidal currents regularly expose the sediments [Michallet *et al*., 2009]. In addition, breaking waves can inject air bubbles into the nearshore sediments. Few of the UXO remediation sites of interest are located in the intertidal zone. Outside of the intertidal zone, much gas content is biogenic in origin (largely methane) [Jackson and Richardson, 2007], however fine-grained, organic-rich sediments are not typical for high-energy environments where liquefaction is expected to play a role.

Air/gas content in soils has long been an issue for debate. It is challenging to make direct measurements within in-situ sediments, so some studies have inferred gas content indirectly, with Tørum, [2007], reporting values about $S_r = 0.97$ from air content trapped in the pores of a sandy seabed not influenced by draining at low tide. In laboratory experiments, normal sand bed preparation resulted in $S_r = 0.96$, while special flushing techniques with de-aired water were required to reach a high degree of saturation at $S_r = 0.99$ [Chowdhury *et al*., 2006]. Most studies focusing on residual liquefaction make the assumption that the sediment is fully saturated ($S_r = 1.0$), conditions under which momentary liquefaction does not happen. Evidence of gas presence in sandy sediments has not been evident in sediment acoustic propagation, whereas bubbles are demonstrated in organic-rich sediments.

As presented in Section 2.1, the solution for liquefaction response becomes more complex for a finite thickness seabed, i.e. a thin layer of porous sediment overlying an impermeable substrate. Many practical analyses, particularly laboratory experiments concerned with engineering failures, have been applied in layered environments [Sumer, 2014a], where two length scales are required: d, the water depth and h, the thickness of the porous seabed, illustrated in Figure 2.1. In the real-world setting of munitions management, the coring and seismic surveys necessary to evaluate the

thickness of the site seabed will not generally be available, and *h* may be unknown. When *h* is a significant portion of the water wavelength L, (approximately when *h*/L > 0.3), then the Hsu and Jeng [1994] solution for finite soil thickness converges with the Yamamoto *et al.* [1978] equations for h = ∞. For application in UnMES, storm waves (typically wave periods T from 7 to 16 s) in the nearshore (water depth *d* < 10 m) have a range of L between 50 to 150 m, so that *h* > 45 m can be treated as effectively infinite.

In practical applications, prediction of liquefaction response is hindered by imprecise knowledge of sediment properties. Environmental surveys to measure properties of the seabed can be undertaken using conventional laboratory tests of bored samples. However, there are multiple difficulties, including disturbances of the sediment caused by sampling; and difficulty controlling the degree of saturation in sand samples [Jeng, 2003]. In situ field measurements prove more accurate, but are laborious and expensive. Previous efforts to account for these large unknowns include neural network modeling [Rahman and Wang, 2002] that used fuzzy classification emphasizing that liquefaction is a continuous process with gradual transition between states.

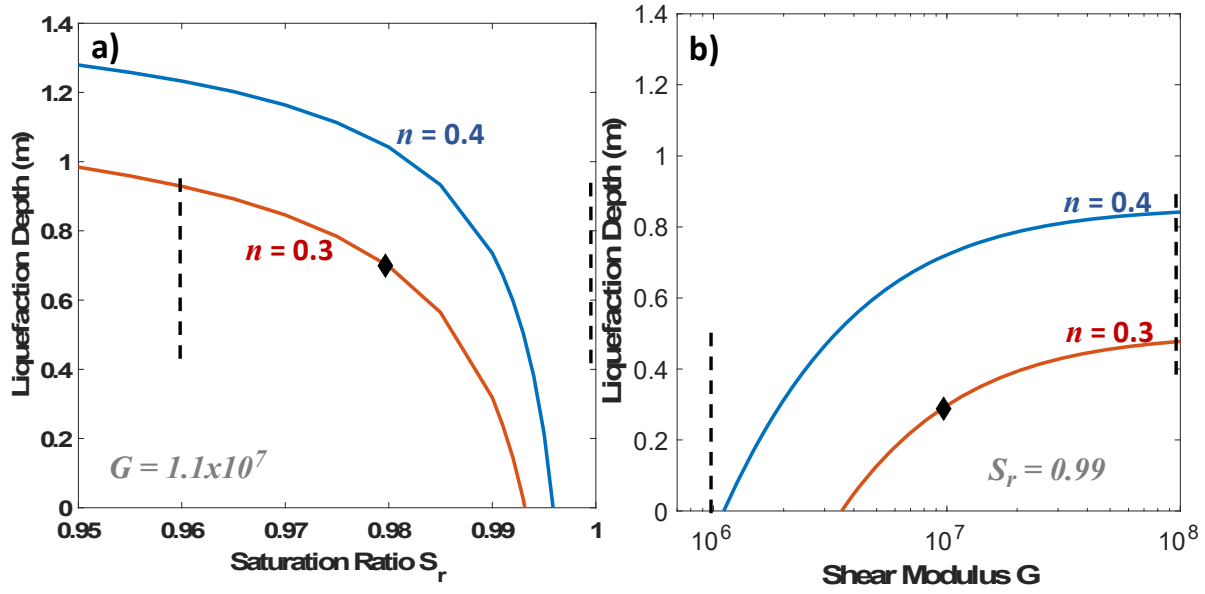

Figure 2.2. Maximum depth of liquefaction z_L computed over a range of a) saturation ratio S_r, and b) shear modulus G for two porosities (*n*). The black diamonds mark the baseline settings for S_r and G used in Klammler *et al.*, [2020] discussed in Section 2.3, and the dashed lines mark the maximum and minimum values considered in their sensitivity studies.

The Bayesian network approach of UnMES allows each parameter to be a probability distribution rather than a single value, thereby accounting for the uncertainty. It is important to understand sensitivity of results to each of the environmental parameters, and focus on the most influential ones. Figure 2.2 illustrates the sensitivity of maximum depth of momentary liquefaction z_L for saturation ratio S_r and shear modulus G over the range of possible values discussed above. These

example dimensional results are calculated from the simplified equations of Qi and Gao [2015] (discussed in the following section) for large storm waves (H_s = 3.5 m, T = 13 s) in the surf zone (d = 6 m). Liquefaction depth is shown for two porosities (n = 0.3 and 0.4). The range of G best representative of fine to medium sand is between the two dashed black lines in Figure 2.2b. The saturation value will vary with the site, depending on tidal conditions and benthic biology, along with other poorly know factors, but coastal sandy sites offshore of the tidal zone will likely have $S_r > 0.99$. The extreme sensitivity of z_L in this S_r range ($0 < z_L < 0.8$ m) diminishes the value of predicting momentary liquefaction unless onsite measurements of soil gas content can be obtained.

Approaches to characterizing the sediment parameters for input for UnMES could make use of research into determination of structural seabed properties from surveys of acoustic-seafloor interaction [Heffner, 2015, Jackson and Richardson, 2007]. Acoustic propagation in sediment depends on many of the same physical properties. In particular, acoustic scattering is highly sensitive to sediment gas content. There are empirical relationships developed to estimate a number of sediment properties from more easily determined measurements such as grain size distribution [Richardson and Briggs, 2004]. Given the sensitivity exhibited, relying simply on the median grain size is insufficient; there is evidence that sand with even a small amount of clay content will be substantially more likely to generate excess pore pressures under waves [Sumer, 2014b].

2.3 Liquefaction Studies Relevant to Object Burial in Non-cohesive Sediment

The majority of research into wave-driven liquefaction has been driven by engineering concerns for the failure of large marine structures. There have been few studies specific to the potential for individual objects to migrate vertically in liquefied sediment. Following is a summary of the salient findings in the limited literature, including SERDP supported studies, on object burial due liquefaction under wave action relevant to process modeling in UnMES.

A seminal paper by Sumer *et al*. [1999] reported on laboratory experiments in a wave flume that reproduced field observations where pipelines or objects such as concrete blocks migrate vertically through the sediment when the strength of the soil is reduced due to the build-up of pore-water pressure. The experiments used a sediment layer of unconsolidated silt, so the progressive, residual liquefaction mechanism was dominant. The results relevant to application in UnMES showed that the objects can sink into the bed or float to the seabed surface depending on its specific density, S_{obj}. The value of specific density leading to sinking for pipelines appeared to be around $S_{pipe} > 1.3$, smaller than the expected value near $S_{liq} \sim 1.8$, the specific density of completely liquefied soil. Pipes were observed to sink to a depth of 2 - 3 diameters, although low density pipes ($1.3 < S_{pipe} < 2.0$) stopped sinking at relatively shallower depths, suggesting that the liquefied soil becomes denser with increasing depth. A later review by Sumer [2014b] verified the relationship

$S_{liq} = 0.18\, z/d + 1.85$, and concluded that in order to sink, the density of an individual object needs to be higher than that observed for pipelines, more like $S_{obj} > 2.0$. The sinking of a spherical object appeared limited only by the thickness of the initially unconsolidated layer.

Much of the early applied work on liquefaction focused on low permeability, very fine-grained beds such as silt or silty sand; there being a general perception that excess pore-pressure did not play any important role in non-cohesive sediments [Sumer, 2014b]. However, a laboratory study by Liu *et al.* [2015] clearly demonstrated wave-induced momentary liquefaction conditions in a sand bed with excess pore-pressure exceeding the overburden pressure according to Criterion B in Section 2.1. Maximum liquefaction depths were measured between $0.4 < z_L < 1.0$ m , under a range of wave characteristics, sand densities and saturation. The laboratory sand bed had a finite thickness (h = 1.8m), and the analytic solution of Hsu and Jeng [1994] successfully reproduced the measured vertical pore pressure distribution.

The Mei and Foda [1981] boundary layer solution was used by Sakai *et al.,* [1992] to explain observations of the sinking of concrete armoring blocks into a sand bed under wave action. Under surf zone conditions, where wave heights approach $H_s \sim 0.75*d$, the Sakai *et al.,* [1992] expressions compute quite deep liquefaction depth in sand, with z_L approaching half the wave height, $z_L \sim 0.5*H_s$. It was assumed the armored sand bed characteristics could be represented by $S_r = 0.99$, $G = 1x10^8$, and $n = 0.33$. For comparison to Figure 2.2, which represents wave forcing with $H_s \sim 0.5*d$, Sakai's approach estimates z_L at about $0.3*H_s$, which is still deeper than the Qi and Gao [2015] results plotted. The Sakai *et al.,* [1992] equations were implemented during the ONR Mine Burial program to predict liquefaction burial [Elmore and Richardson, 2004], however high-energy burial in sand was not demonstrated by additional observations.

The SERDP-sponsored experiment DUCK15 provided some of the only field observations on UXO burial related to liquefaction [Calantoni, 2017]. The surrogate UXO were deployed in d = 6 and 8 m offshore of the FRF at Duck, NC, and ranged in diameters from 0.025 to 0.155 m, with specific densities $2.6 < S_{obj} < 7.6$. Following a strong storm (peak waves with H_s = 3.5 m, T = 13 s), measurements of burial depths between 0.1 to 0.6 m were made by diver observation, plotted in Figure 2.3a versus density as S_{obj}/S_{water}. Measurements by divers are inherently imprecise, especially for the small, bullet-like surrogates (shown as blue asterisks), so that the vertical position is best considered to be known ±0.05 m. The UXO diameter D_{obj} is indicated by the height of the vertical bars at each symbol. Altimetry from a quadpod measurement system co-located at the 8 m site revealed no far-field seabed elevation change, confirming that the UXO burial was a local process. Relative burial depth (burial depth/UXO diameter, or B_{obj}/D_{obj}) is shown in Figure 2.3b, and reveals an interesting trend of increasing burial as a function of object density, in this case plotted relative to the bulk sediment density as S_{obj}/S_{sed}.

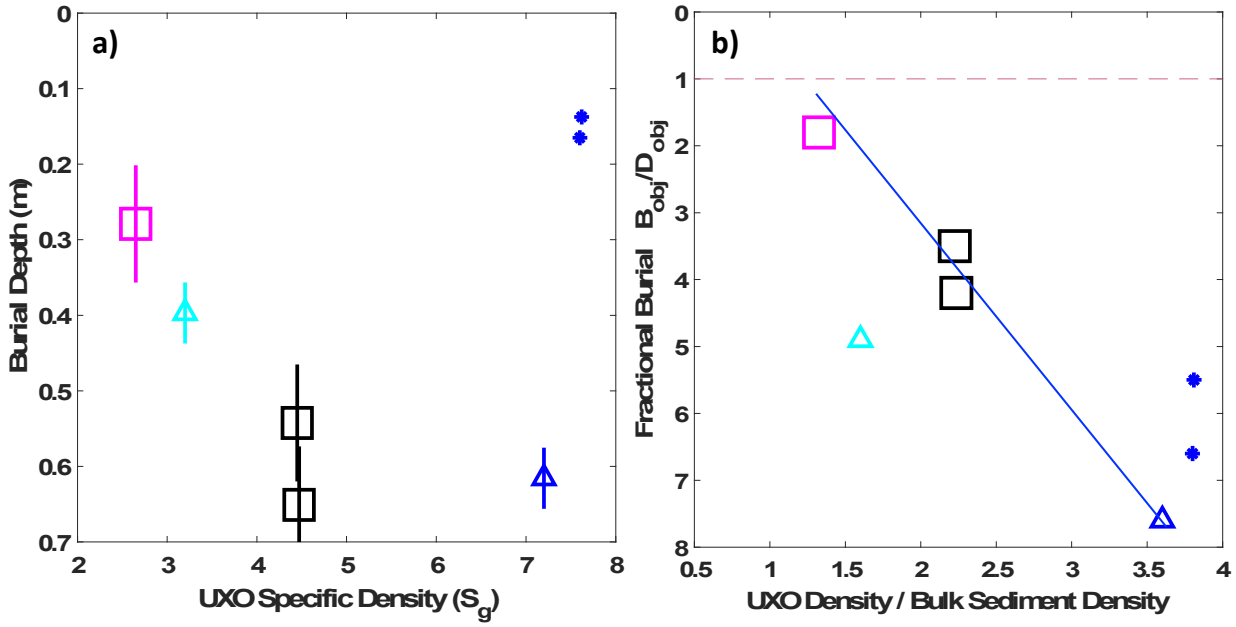

Figure 2.3 Observations of UXO burial from DUCK15 [Calantoni, 2017] presented dimensionally (a) and as relative burial (b) versus the density of surrogate UXO used in the field test. Slope of blue line provides estimate of duration divided by friction coefficient

Recent work by Klammler *et al*. [2020] applied the Hsu and Jeng [1994] equations in an analysis of momentary liquefaction for field conditions during DUCK15. Using the wave characteristics measured at the peak of the storm, zones of sediment instability were calculated within the seabed. A number of different sediment failure criteria were considered to determine onset of the liquefied state, including two that are equivalent to Criteria A and B defined in Section 2.1. Most of the important sediment and pore water properties discussed in Section 2.2 were not measured for the DUCK15 field test; however, a set of best estimate values were chosen appropriate to fine to medium-grained sand, and used in the Hsu and Jeng solution. The burial depth to which the surrogate UXO would settle was calculated depending on the length of time during momentary sediment instability, as well as its maximum failure depth z_L defined by the various failure criteria. The calculations z_L of based on Criteria A and B were indistinguishable, and matched the DUCK15 observed maximum burial depth of ~ 0.6 m more closely than the other proposed failure criteria.

Acknowledging the sensitivity of equation coefficients to the unknown soil and pore water characteristics, Klammler *et al*. [2020] also calculated z_L results calculated by varying each important parameter to its minimum and maximum value expected for sand. With the baseline depth using best estimate values calculated as $z_{Lbase} = 0.56$, the failure depths calculated over the possible range for several parameters varied from $0 <= z_L < 2\ z_{Lbase}$. As expected, the highest sensitivity was due to the uncertainty range for saturation and shear modulus, as plotted in Figure 2.2 where the baseline values are marked with black diamonds, and the minimum and maximum values used for S_r and G are delineated by dashed black lines. The uncertainty range considered by Klammler results in z_L estimates covering much of the z_L range exhibited by different failure

criteria, so that conclusions about the operative mechanism for sediment instability are difficult to support, given the acknowledged parameter uncertainty.

The Hsu and Jeng [1994] finite-layer model is complex, requiring the evaluation of over 100 terms. The sediment layer thickness h at the DUCK15 field test site was not known (except that $h > 6$ m, based on previous sediment cores at the site). The baseline case in Klammler *et al*. [2020] assumed $h = 100$ m, so that $h/L \gg 0.3$, therefore h is large enough to be treated as infinite (Jeng *et al.* [2007], see Section 2.2). In fact, among the parameter sensitivity tests reported, the calculation with $h = \infty$ results in $z_L = z_{Lbase}$. An alternative approach would be to compute excess pore-pressure with the widely-used solution for infinite h from Yamamoto *et al.* [1978], which is substantially simpler to implement. Given the uncertainty due to poorly known sensitive parameters, the high complexity of the Hsu and Jeng may not be justified in an operational application like UnMES.

The Yamamoto analytic model is the basis for a sequence of investigations by Qi and Gao [2015, 2018] into momentary liquefaction under waves in non-cohesive sediments. Qi and Gao simplified the solution further using the 1-D approximation for the pore-pressure solution developed by Chowdhury *et al.* [2006], who showed that the 1-D approximation was very similar to the 2-D solution in the upper half of the sediment layer. Applying a modified version of Criterion C for the threshold of sediment instability, assuming that the soil particles in the liquefied layer should be in an exact suspended state, Qi and Gao derived an expression for the maximum momentary liquefaction depth z_L under the trough of a wave with seabed amplitude $P_{b(max)}$:

$$z_L = \frac{P_{b(max)}}{(\gamma_s - \gamma_w)} - \frac{1}{a(1-B)} \qquad \text{Eq.(1)}$$

where the coefficient $a = \text{sqrt}\,(w/2\boldsymbol{C}_v)$ is the complex vertical wave number within the bed, with $B = 1/(1+n\beta/\boldsymbol{m}_v)$ a compressibility coefficient, and $w = 2\pi/T$ is the wave radian frequency. Additional combined parameters are $\boldsymbol{C}_v = k_z B/\boldsymbol{m}_v\gamma_w$, the sediment coefficient of consolidation, and $\boldsymbol{m}_v = (1/E)[1\text{-}2\nu^2/(1\text{-}\nu)]$, the volumetric compressibility of soil. The other terms are as defined in Section 2.2. Qi and Gao found that their modified z_L lies in between the maximum liquefaction depths determined by Criteria B and C, and emphasized that all calculations are strongly dependent on S_r.

Friedrichs [2018] applied this Qi and Gao solution to predict the maximum depth to which an object could sink into the seabed due to liquefaction (z_L). Over time, the burial depth of an object B_{obj} will approach z_L. However, the time scale required to sink to z_L is not well known. Many earlier investigations assumed that objects will move rapidly through the liquefied sediment, as in Klammler *et al.* [2020] where a sinking velocity v_{sink} on the order of 1 m/s was used. With this assumption B_{obj} will rapidly equal z_L, and Klammler compared computed z_L only to the deepest burial in the DUCK15 observations. The densities of the surrogate UXO were not taken into

account, although the DUCK15 data showed UXO buried to different depths according to their density (Figure 2.3b).

Other studies have suggested much slower sinking velocity. Laboratory experiments in a 1-D facility measuring the sinking process for objects of two different densities in liquefied sand were reported by Chowdhury *et al.* [2006]. Because momentary liquefaction occurs only during a part of the wave phase, the objects were observed to sink and stop alternately. The measured rate of sinking during was extremely slow ($v_{sink} \approx 10^{-5}$ m/s), noting that the density of the object used was fairly light, $S_{obj} = 2.4$. Kirca [2013] performed experiments in a larger wave-flume facility looking at sinking of objects driven by residual liquefaction in silt. The experimental objects had with a wide range of density with $1.9 < S_{obj} < 8.9$. Kirca's measured velocities for v_{sink} were on the order $\approx 10^{-3}$ m/s. A force balance analysis of the object's velocity was presented that showing estimated drag coefficient C_D ranging over 2 orders of magnitude given the unknown range of viscosity in liquefied soil.

Friedrichs [2018] explored a similar force balance between buoyancy and drag, formulating the latter in terms of a friction coefficient $\boldsymbol{f_c}$ after Clement, *et al.* [2018]. Assuming the drag force balances the buoyancy force as the object sinks, the equation for sinking velocity becomes

$$v_{sink} = \frac{D_{obj}}{\boldsymbol{f_c}} \left(\frac{S_{obj}}{S_{sed}} - 1\right), \qquad \text{Eq.(2)}$$

where the D_{obj} is the diameter of the object, S_{obj}, S_{sed}, are the specific densities of the object and bulk sediment, respectively. (This solution also works for the velocity at which an object would rise if S_{obj} is less than S_{sed}.) Assuming that the burial depth of an object B_{obj} can be computed by integrating v_{sink} over the duration of the liquefaction event T_L, Friedrichs proposed to estimate $\boldsymbol{f_c}$ based on the observations from DUCK15. Combined with the Qi and Gao [2015] estimation of z_L, this pragmatic approach was used for the prototype implementation of a momentary liquefaction burial model in UnMES discussed in Section 4. Recently, this simple method was reviewed, and an improved viscous approach examined, to explain the observed burial depths [Wang *et al.,*2020]. A time sequence of wave data can be used; z_L changes with the wave forcing, so that change in object burial is calculated at each time step (for details see Section 4). Applying this iterative burial model to the DUCK15 wave data, using assumptions regarding the seabed soil properties, reproduces burial depths in good agreement with the observed burial data from DUCK15, accounting for the varying S_{obj}.

Acknowledging at the empirical estimation of $\boldsymbol{f_c}$ from limited field data to be unsatisfactory for wider application, Wang *et al.* [2020] focuses on determining effective viscosity μ of liquefied sediment in order to estimate the drag force. A comprehensive summary of existing literature estimating μ was reviewed, with reports of μ of liquefied sand in a wide range, from 1 to 6000

kPa-s. Theory suggests that viscosity should depend on parameters such as relative density D_r, but this was not evident in the data summary. Wang points out that apparent viscosity varied under different experimental conditions, coming to a similar conclusion as Kirca [2013] that liquefied sand may act as a shear-thinning non-Newtonian fluid where μ decreases with higher shear strain rate. Because momentary liquefaction occurs only during part of the wave phase, the sediment will alternate between unstable and stable; v_{sink} varies throughout each wave, slowing to zero under each wave crest as the sand is stabilized by the increased downward pressure. Given current knowledge, there are too many details unknown to accurately determine time-varying sinking on an object, so that estimation of a bulk v_{sink} as a steady velocity is an expedient simplification (see Section 4).

2.4 Summary of Observations of Burial by Momentary Liquefaction

Studies and data directly relevant to burial of UXO-like objects by liquefaction are extremely limited. The SERDP-sponsored field work of Calantoni (MR-2320) from DUCK15 has yielded a half-dozen observations that demonstrate high-energy wave-driven burial into sand in the nearshore region. As discussed in the previous section, these data points have been used extensively for verifying liquefaction model results. Other frequently cited field observations come from a macrotidal beach in southwest France subject to high energy waves [Mory *et al*., 2007, Michallet *et al*., 2009]. Although object burial during liquefaction was not part of these experiments, extensive measurements of pore pressure, sediment geotechnical properties, and gas content allowed for a clear demonstration of momentary liquefaction events that commenced and dissipated within one wave period. The seabed was liquefied down to depths of 0.3 to 0.5 m, with evidence that Criterion C was the most appropriate threshold to indicate instability. Because the test site was exposed to the air during low tide, the gas content was high; there was very low saturation, with $S_r \sim 0.94$, even lower than considered in the sensitivity study shown in Figure 2.2a. However, note that conditions in this macrotidal environment, with sandy sediments daily exposed to the air, are not applicable to most of the UXO remediation sites of interest.

SERDP project MR-2731 proposed using surrogate munitions with embedded pressure sensors to measure the pressure fluctuations of momentary liquefaction [Foster and Gillooly, 2017]. Such pressure-mapped munitions have been developed and were deployed in nearshore environments, however no conditions conducive to liquefaction were observed: either the wave energy was too low, or the coarse sediment had such large permeability than the pore pressure could drain rapidly. Another project, MR-2503, conducted a number of investigations in the high-energy swash-zone [Puleo *et al.,* 2017] where liquefaction mechanism may play a role. However, pore pressure in the beach face was not measured, and the complexity of forcing and UXO behavior under breaking waves is such that the contribution of liquefaction would be difficult to distinguish. Evidence of

shear-stress generated bed fluidization was determined to be a more likely explanation for the swash zone observations of deep burial ($B_{obj}/D_{obj} > 1$) [Cristaudo and Puleo, 2020].

In summary, the measurements from the DUCK15 provide the only current field evidence of object burial by the liquefaction mechanism. However, the data set obtained in this study is very limited so that comparisons of liquefaction burial models are not satisfactory for model validation proposes. On-going SERDP studies, discussed in Section 5, hold the promise of improved understanding, but at present there remains a lack of adequate data as well as an insufficient level of model validation to justify further implementation of the liquefaction burial mechanism in UnMES. Thus, a NO-GO decision regarding inclusion of liquefaction models in the expert system at this time is appropriate.

3. Granular Sorting Process

Burial of UXO in cohesive and fine sand bedforms can result from other processes than liquefaction, such as granular sorting (convection and/or segregation) as well as direct sinking due to the density disparity between the UXO and the bulk sediment.

Granular convection, or granular segregation, is a phenomenon where granular material subjected to shaking or vibration will exhibit circulation patterns similar to types of fluid convection. It is sometimes described as the Brazil nut effect when the largest particles end up on the surface of a granular material containing a mixture of variously sized objects [Rosato *et al.*, 1987]. The terminology derives from the example of a typical container of mixed nuts, where the largest will be Brazil nuts. Under experimental conditions, granular convection of variously sized particles has been observed to form convection cells.

Granular sorting generally results from shaking the medium, generally horizontally, so that an object gets displaced. In situations where the sediment is highly unconsolidated, e.g. loose grains where the object and sediment densities are about the same, the small grains will fill in the void space under the bigger object(s) and they will move up – i.e. the Brazil nut effect. The potential for this phenomenon to re-expose UXO previously buried in sand is of great interest in remediation studies; however, no field evidence yet supports this. In general, both object size and density play a role. If the sediment is saturated or partially saturated, the weight of the object will let it sink, to the depth where the submerged density (dry density minus that of the displaced sediment) equals the sediment density, e.g. quicksand. In this situation the object shape does not matter, only its density. The reverse Brazil nut effect will move large particles to the bottom if they are much denser than the smaller particles [Hong *et al.*, 2001]. Calantoni [2018] suggested that this mechanism could be an alternate explanation for the deep and density stratified burial of UXO observed during DUCK15; however, no first-order process model suitable for use in UnMES is currently available that captures these proposed physics.

3.1 Granular Sorting Studies Relevant to UXO Burial.

Clément *et al.* [2018] performed experiments on the sinking of spherical objects in various bedform compositions due to horizontal vibrations of the bedform. The burial depth varied as a function of the object density and seabed composition. The results of this study, with its focus on high-frequency ground acceleration due to earthquakes, do not provide clear guidance for modeling ocean wave-driven UXO burial.

Lohse et al. [2004a, 2004b] performed a limited series of experiments where a small heavy sphere was dropped into a loosened, pre-aerated, sand bed. It was found that the depth of penetration of the spheres as directly proportional to the sphere mass, with the constant of proportionality related to the specific properties of the sand bed. The burial mechanism is, in this case, one of density sorting upon impact or release of the object rather than liquefaction. These experiments showed that the final object depth is related to its density, which is in agreement with the Calantoni [2017] field observations. However, the penetration observed by Lohse may be dominated by the impact penetration rather than the looseness of the sand bed, so that the relevance of these observations to storm-driven UXO burial is not clear. The operative process during the DUCK15 experiment may well be granular sorting rather than liquefaction, however the limited scope of the DUCK15 data and the paucity of other relevant data make this determination quite tentative.

In general, it is found that knowledge of object displacement by granular sorting mechanisms is at present insufficient to model UXO burial and assess the model viability. It is noted that studies observe variation in convection patterns excited by different frequencies and direction of vibration so that it is unlikely that conclusions drawn from the more prevalent seismic studies can be applied to ocean wave-induced sediment shaking. The distinction between granular sorting and liquefaction is not, at present, sufficiently clear due to the paucity of studies of object burial, especially studies under actual field conditions.

4. Implementation of Liquefaction Modeling UnMES

As liquefaction and granular sorting mechanisms can potentially cause UXO burial, they ultimately need to be included in UnMES. It has been found that the extant literature on burial of isolated objects analogous to UXO driven by these processes is very limited. Currently, funded SERDP-MR efforts are designed to investigate these burial mechanisms. These studies are currently in progress and hold the promise of greatly improved understanding. However, at present, there is an insufficient level of knowledge, as well as the lack of adequate data and models to justify operational application. Thus, at this time a NO-GO decision regarding full implementation of high-energy liquefaction and granular sorting process models in UnMES is appropriate. For research purposes, the model to estimate final burial depth presented by Friedrichs [2018] and Wang *et al.* [2020], as discussed in Section 2.3, is implemented in UnMES as a

preliminary tool, with the required environmental parameters represented by probability distributions.

The momentary liquefaction model of Qi and Gao [2015], based on Yamamoto *et al.* [1978], provides a simple method to calculate maximum depth z_L, given specification of the wave conditions and sediment characteristics. If an object such as a UXO does not drop instantaneously to z_L, the remaining question is the bulk rate v_{sink} at which an object does sink down during the moments of sediment instability.

Assuming that the burial depth of an object B_{obj} can be computed by integrating v_{sink} over the duration T_L of the liquefaction event, Friedrichs proposed to estimate the frictions coefficient $\boldsymbol{f_c}$ in Eq. (2) from the DUCK15 observations. Using wave measurements at the Duck field test in February 2015 during which the surrogate UXO became buried, calculation of Eq. (1) showed that $z_L > 0$ during the peak of the storm for a duration $T_L \sim 35$ hours. Assuming $B_{obj} = v_{sink} T_L$, and using Eq. (2), the ratio $T_L/\boldsymbol{f_c}$ can then be estimated from the field observations presented in Figure 2.3b with

$$\frac{B_{obj}}{D_{obj}} = \left(T_L/\boldsymbol{f_c}\right)\left(\frac{S_{obj}}{S_{sed}} - 1\right) \qquad \text{Eq.(3)}$$

A reasonable fit to the DUCK15 data gives $T_L/\boldsymbol{f_c} \approx 8/3$, as indicated by the blue line in Figure 2.3b. Using $T_L \sim 35$ hours, the value assigned to $\boldsymbol{f_c} \approx$ 13 hours.
Liquefaction depth z_L varies with time t as the wave forcing changes, so that the object burial is calculated at each time step. Object sinking in wave period i is determined iteratively by:

$$\begin{aligned} \Delta B_{obj(i)} &= \frac{D_{obj}}{\boldsymbol{f_c}}\left(\frac{S_{obj}}{S_{sed}} - 1\right)\Delta t(i) \qquad \text{if } B_{obj(i)} < z_{L(i)} \\ \Delta B_{obj(i)} &= 0 \qquad\qquad\qquad\qquad\quad \text{if } B_{obj(i)} \geq z_{L(i)} \end{aligned} \qquad (4)$$

in which $\Delta B_{obj(i)}$ is the change in burial within the present wave measurement time step $t(i)$. The final depth B_{obj} is then simply the sum of all incremental values of $\Delta B_{obj(i)}$:

$$B_{obj} = \sum_{i=T_{L0}}^{T_L} \Delta B_{obj(i)} \qquad \text{Eq. (5)}$$

The time T_{L0} designates when the storm peak first arrives, i.e. when the wave energy grows large enough so that $z_L > 0$.

For implementation in UnMES, several burial processes are considered during the storm event. Scour is frequently acting to bury the UXO even under moderate waves [Friedrichs *et al.*, 2016].

The Monte Carlo code that generates the training cases to build the burial node's CPT in UnMES generates many storm sequences. The peak wave height H_s for a given sequence is drawn from a uniform distribution of allowable heights given the local water depth d, noting the wave breaking will decrease the upper limit of H_s as d shoals inshore. Another random draw provides a value for the wave growth rate, a measure of how quickly the storm moves into the area [Traykovski, 2017]. The duration of the storm sequence is then based on statistics from Dolan and Davis [1992], amended to count for the wave growth rate, and imposing a minimum duration for the events with smaller H_s. The wave growth and decay over the storm sequence is schematized using a pattern recommended by Poelhekke *et al*. [2016], resolved with a time step of 1/2 hour.

During this synthetic storm event, scour will generally initiate UXO burial, designated as B_{scour}. The threshold to compute high-energy processes is passed when the Shields parameter θ becomes large ($\theta > 1$) indicating that sheet flow conditions prevail [Sumer e*t al*. 1999], or if H_s exceeds the wave breaking criteria. When high-energy conditions begin, the implemented code passes the scour burial computed so far, $B_{obj(i=TL0)} = B_{scour}$, to initiate the iterative procedure in Eq. (5).

There are multiple sources of error and uncertainty in this proposed procedure to model UXO burial due to liquefaction, notably the somewhat *ad hoc* estimation of friction coefficient controlling v_{sink} . Investigation into replacing $\boldsymbol{f_c}$ with an improved physics-based specification of viscosity is currently being pursued both by Wang *et al.* [2020] and Klammler *et al.* [2021]. It is also clear from Figure 2.2a that lack of precise knowledge of the saturation ratio S_r in the sediment can change the value of z_L by 100%. Successful comparison of computed B_{obj} to the DUCK15 observations, as presented in Wang *et al.* [2020] was achieved by using S_r essentially as tuning parameter, assigning a high saturation to the seabed, $S_r > 0.99$, a region where changes even in the third decimal place of S_r change the results for z_L dramatically. As such, this liquefaction model can act as a placeholder in UnMES, but is not to be considered validated. Lacking validation, the liquefaction predictions should not be used as guidance by remediation site managers.

Even with improved understanding of the physics, the important environmental measurement will generally not be well known. In the face of such large input uncertainty, it is appropriate when building UnMES with the MC exploration of the storm event parameter space, to treat the value of S_r as a random variable. The same procedure can be applied to assigning a value to the shear modulus G. An example is shown in Figure 4.1 for wave conditions representative of the peak of the DUCK15 storm at the observation site where d = 8 m. For $S_r = 0.99$, with $n = 0.4$ and $G = 1.1 \times 10^7$, the implemented code predicts $z_L = 0.5$ m (marked as red bars). Representing only a portion of the acknowledged uncertainty in environmental inputs, saturation is then drawn from a normal distribution with mean $S_r = 0.99$, and a fairly narrow variance ($\sigma = 0.0025$), with all the other sediment and pore water parameters were held fixed. Even with this modest uncertainty in a

single parameter, the predicted liquefaction depth exhibits a broad spread (Figure 4.1b), including a significant percent of cases where no liquefaction burial is predicted to occur.

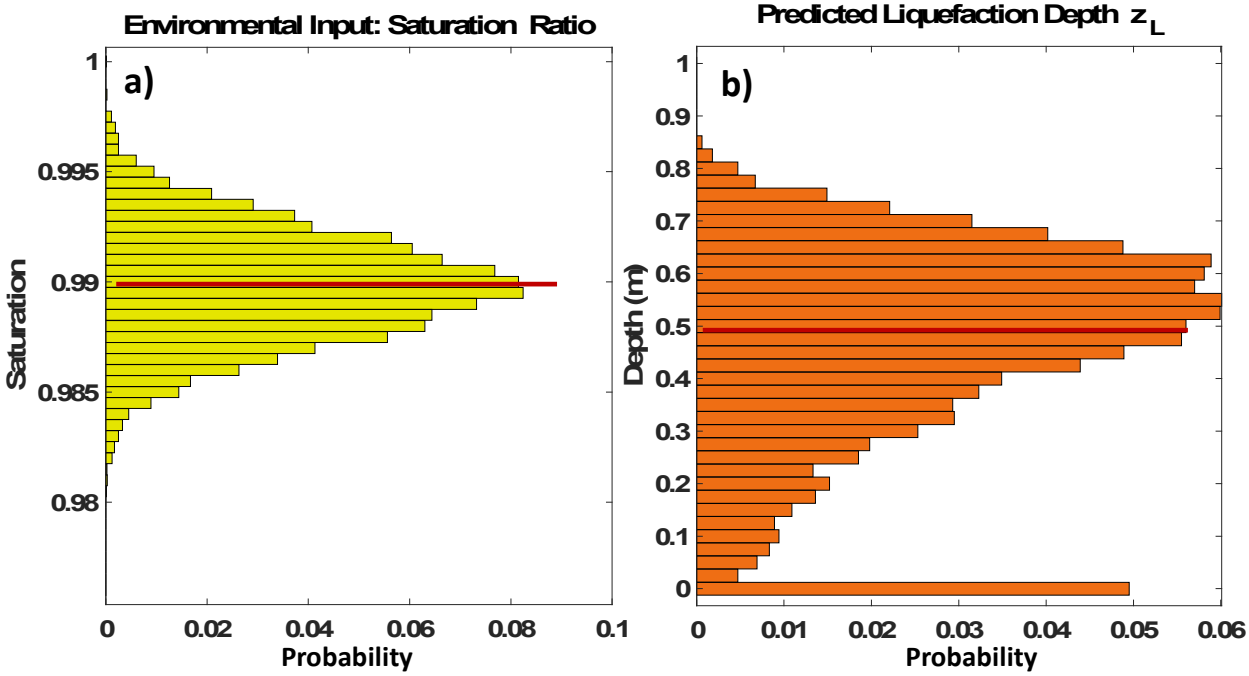

Figure 4.1 Normal distribution of a) saturation ratio represents uncertainty in sediment parameter, which results in a wide distribution of b) predicted liquefaction depth.

5 Summary and the Way Forward

As liquefaction and granular sorting mechanisms can potentially cause UXO burial, they are important processes to capture in the underwater munitions expert system. There is extensive literature investigating seabed liquefaction, with a portion of it focused on the wave-driven momentary liquefaction process relevant to UXO burial in coastal sites. However, there are a limited number of studies considering the behavior of individual objects within liquefied soil. There is reasonable modeling capacity to estimate the depth to which the seabed will become unstable under liquefying conditions if the thickness of the seabed is large; modeling response in thinly layered sediments is substantially more difficult. How UXO bury in momentarily unstable sediment is poorly known, with strongly varying estimates of the effective drag, and time scale of sinking. However, the main obstacle to predictive utility of liquefaction modeling appears to be the strong sensitivity to seldom-measured sediment and pore water properties. In particular, the evidence for air content in sandy sediments of interest has not been established. If, in general, coastal non-cohesive sites are completed saturated, then the role of momentary liquefaction in sand is very limited.

Currently funded SERDP-MR efforts are designed to further investigate these burial mechanisms. Foster [MR-2731] has developed pressure-mapped munitions which can measure in-situ the local pressure changes concurrent with UXO vertical movement for detailed understanding of burial behavior. However, it is not clear whether the planned field work under MR-2731 will include conditions conducive to liquefaction. Calantoni and Penko are collaborating under MR-2320 and MR-1317 with geotechnical engineers at the University of Florida to build "smart" surrogate munitions with sensitive pore pressure and stress sensors, and to develop their Dynamic Seabed Burial Model for predicting the final burial depth of an object. They propose that liquefaction degree (R, discussed in Section 2.1) can be established as having a simple dynamical relationship with acoustic backscatter [Klammler *et al.,* 2021]. Since acoustic backscatter is readily measured, validation of this relationship would be an important advance in making an operationally viable liquefaction model.

These on-going SERDP studies show promise to improve ability to predict UXO burial due to high-energy processes. But at present, operational predictions are likely to be overwhelmed by uncertainty. One aspect of UnMES is its ability to provide guidance to remediation site management making decisions about where they need to invest in environmental measurements. If the spread in burial prediction is too broad to be of use in management decisions, then obtaining improved input information may be a high priority. However, in the case of current liquefaction burial modeling, the uncertainty in the single environmental input illustrated in the Figure 4.1 example is just a small part of the total uncertainty. In addition to the other sediment parameters discussed in Section 2.3, uncertainty in the drag forces that affect the rate of sinking for an object in liquefied sediment should be accounted for. If all these sources of uncertainty were taken into account, the resulting predicted burial would likely approach a uniform distribution, providing no information. Given this situation, further efforts to validate of the current UnMES implementation are not warranted. Thus, a NO-GO decision is made for further development of UnMES to implement the liquefaction and granular sorting process models available at this moment.

A meeting of the research teams to clarify processes descriptions and terminology would be useful. At this meeting, the necessary physical models, process interactions, and field and laboratory data required for validation could be agreed upon. At some time in the near future, further laboratory and field observations of UXO burial under high-energy conditions hopefully will clarify the aspects of the processes that are now unclear, and allow validation of useful models that reproduce a significant portion of the burial behavior.

References

Biot, MA, 1956. "Theory of propagation of elastic waves in a fluid-saturated porous solid, Part I: Low frequency range," J. Acoust. Soc. Am. 28, 168–177.

Calantoni, J. 2017. "Long Time Series Measurements of Munitions Mobility in the Wave-Current Boundary Layer," SERDP In-Progress Review, May 2017.

Calantoni, J. 2018. "Long Time Series Measurements of Munitions Mobility in the Wave-Current Boundary Layer," SERDP In-Progress Review, May 2018.

Clément C, Toussaint R, Stojanova M, Aharonov E, 2018. "Sinking during earthquakes: Critical acceleration criteria control drained soil liquefaction," *Phys. Rev. E 97*, 022905.

Chowdhury B, Dasari GR, Nogami T, 2006. "Laboratory Study of Liquefaction due to Wave–Seabed Interaction," *J. Geotech. Geoenviron. Eng., 132*(7): 842-851.

Cristaudo, D, Puleo JA, 2020. "Observation of munitions migration and burial in the swash and breaker zones," Ocean Engineering, Vol 205, 107322, 2020.

Dolan, R, RE Davis, 1992, "An Intensity Scale for Atlantic Coast Northeast Storms," Journal of Coastal Research, Vol. 8, No. 4 (Autumn, 1992), pp. 840-853.

Elmore, PA, M D Richardson, "Regional mine burial prediction using Monte Carlo and deterministic methods", Proc. 6th Int. Symp.Technol. Mine Problem, Monterey, CA, 2004.

Foster DL, S Gillooly, 2017. "Resolving the Role of Dynamic Pressure in the Burial, Exposure, Scour and Mobility of Underwater Munitions" Project MR-2731, SERDP Burial and Mobility Workshop, June 2017.

Friedrichs, CT, 2018. "Parameterized Process Models for the Underwater Expert System", SERPD Project MR-2647 In-Progress Review, May 2018.

Heffner BT, 2015, "Inversion of High Frequency Acoustic data for Sediment Properties Needed for the Detection and Classification of UXOs," SERDP Project MR-2229 Final Report, 2015.

Hong, DC, Quinn, PV, and S Luding, 2001. "Reverse Brazil nut problem: Competition between percolation and condensation," Physical Review Letters, 86(15), 3423-3426.

Hsu JRC, Jeng DS, and Tsai CP, 1993. "Short-crested wave-induced soil response in a porous seabed of infinite thickness," Int. J. Numer. Analyt. Meth. Geomech. 17(8), 553–576.

Hsu, JRC and Jeng DS, 1994. "Wave-induced soil response in an unsaturated anisotropic seabed of finite thickness," Int. J. Numer. Analyt. Meth. Geomech. 18(11), 785–807.

Jackson D, Richardson M, 2007. *High-Frequency Seafloor Acoustics*, Monograph Series in Underwater Acoustics, Springer.

Jeng DS, 1997. "Wave-induced seabed instability in front of a breakwater", Ocean Eng. 24(10), 887–917.

Jeng DS, 2003. "Wave-induced seafloor dynamics," Appl Mech Rev. 56(4), pp 407-429.

Jeng, DS, Seymour BR, and Li J, 2007. "A new approximation for pore pressure accumulation in marine sediment due to water wave." Int. J. Numer. Anal. Methods Geomech., 31(1), 53–69.

Kirca, VSO, 2013. "Sinking of irregular shape blocks into marine seabed under wave-induced liquefaction," Coastal Engineering, vol. 75, 40–51.

Klammler H, Scheremet A, Calantoni J, 2020. “Seafloor Burial of Surrogate Unexploded Ordinance by Wave-Induced Sediment Instability,” *IEEE Journal of Oceanic Engineering, vol. 45, no. 3, pp. 927-936, July 2020.*

Klammler H, Penko A, Staples T, Scheremet A, Calantoni J, 2021, “Observations and modeling of wave-induced burial and sediment entrainment: Importance of liquefaction degree", in preparation.

Liu B, Jeng D-S, Ye GL, Yang B, 2015. “Laboratory study for pore pressures in sandy deposit under wave loading,” *Ocean Eng., 106,* 207-219.

Lohse D, Bergmann R, Mikkelsen R, Zeilstra C, van der Meer D, Versluis M, van der Weele K, van der Hoef M, Kuipers H 2004a “Impact of Soft Sand: Void Collapse and Jet Formation,” *Phys. Rev. Let, 93,* 198003, 4 pp.

Lohse D, Rauhe R, Bergmann R, van der Meer D 2004b “Creating a dry variety of quicksand,” *Nature, 432,* 689-690.

Mei C.C .and Foda MA ,1981. “Wave-induced response in a fluid-filled poro-elastic solid with a free surface-a boundary layer theory,” Geophys. J. R. Astron. Soc. 66, 597–631.

Michallet, H, M Mory, I Piedra-Cueva, 2009. “Wave-induced pore pressure measurements near a coastal structure.,” J. Geophys. Res. 114 (C6), C06019.

Mory, M, H Michallet, D Bonjean, I Piedra-Cueva, JM Barnoud, P Foray, S Abadie, P Breul, 2007. “A field study of instantaneous liquefaction caused by waves around a coastal structure,” J. Waterw. Port, Coast. Ocean Eng. 133 (1), 28–38.

Poelhekke L., W. S. Jäger, A van Dongeren, TA Plomaritis, R. McCall, Ó. Ferreira, 2016. "Predicting coastal hazards for sandy coasts with a Bayesian Network,” Coastal Engineering 118, pp. 21-34.

Puleo, JA, Bruder, B, Cristaudo,D, 2017. “Quantification of Hydrodynamic Forcing and Burial, Exposure and Mobility of Munitions on the Beach Face,” Interim Report for SERDP Project MR-2503, 2017.

Qi W-G, Gao F-P, 2015. “A modified criterion for wave-induced momentary liquefaction of sandy seabed,” *Theor. Applied Mech. Letters, 5*, 20–23, http://dx.doi.org/10.1016/j.taml.2015.01.004.

Qi W-G, Gao F-P, 2018. “Wave induced instantaneously-liquefied soil depth in a non-cohesive seabed,” Ocean Engineering 153 pp 412-423.

Rahman, MS, Wang, J, 2002. “Fuzzy neural network models for liquefaction prediction,” Soil Dynamics and Earthquake Engineering 22 pp 685–694.

Richardson M, KB Briggs, 2004. “Empirical Predictions of Seafloor Properties Based on Remotely Measured Sediment Impedance,” *High Frequency Ocean Acoustics Conference*, MB Porter and M Siderus (Eds.), AIP, Melville, NY, pp.12-21.

Rennie SE, A Brandt, JG Ligo, 2019. “Prototype Underwater Munitions Expert System: Demonstration and User's Guide,” Johns Hopkins University/Applied Physics Laboratory, FPS-R-19-0695, November 2019.

Rosato A, Strandburg KJ, Prinz, F, and RH Swendsen, 1987. “Why the Brazil Nuts are on top - Size Segregation of Particulate Matter by Shaking,” Physical Review Letters, 58(10), 1038-1040, DOI: 10.1103/PhysRevLett.58.1038.

Sakai T, Hatanake K, Mase H,1992. "Wave-Induced effective stress in seabed and its momentary liquefaction" J. of Waterway, Port, Coastal, and Ocean Eng., Vol. 118, No. 2, 202-206. (Comments and Errata, Proc. J. Waterway, Port, Coastal, and Ocean Eng., Vol. 119,No.6, pp. 692-697, 1993)

Sumer BM, 2014a. *Liquefaction Around Marine Structures*, Advanced Series on Ocean Engineering – Volume 39, World Scientific Pub. Co.

Sumer BM, 2014b. "Advances in Seabed Liquefaction and Its Implications for Marine Structures," *Geotech, Eng. J., 45,* ISSN 0046-5828, 14 pp.

Sumer BM, Fredsoe J, Christensen S, Lind MT, 1999. "Sinking/flotation of pipelines and other objects in liquefied soil under waves," *Coastal Eng., 38,* pp 53-90.

Traykovski, P, 2017. "Continuous Monitoring of Mobility, Burial and Re-exposure of Underwater Munitions in Energetic Near-Shore Environments," SERDP Project MR-2319 Final Report.

Tørum, 2007. "Wave-induced pore pressures—air/gas content," J. Waterw. Port, Coast. Ocean Eng. 133 (1), pp 83–86.

Wang H, Friedrichs CT, Calantoni J, 2020. "Analysis of objects sinking in sand due to momentary wave-induced liquefaction: a viscous fluid approach," *in preparation*.

Yamamoto T, Koning HL, Sellmejjer H, and Hijum EV, 1978. "On the response of a poro-elastic bed to water waves," J. Fluid Mech. 87, 193–206.

Zen K and Yamazaki H, 1990. "Mechanism of wave-induced liquefaction and densification in seabed. Soils and Foundations," vol. 30, No. 4, 90–104.